



HAL
open science

Magnetoresistance of semi-metals: The case of antimony

Benoît Fauqué, Xiaojun Yang, Wojciech Tabis, Mingsong Shen, Zengwei Zhu,
Cyril Proust, Yuki Fuseya, Kamran Behnia

► To cite this version:

Benoît Fauqué, Xiaojun Yang, Wojciech Tabis, Mingsong Shen, Zengwei Zhu, et al.. Magnetoresistance of semi-metals: The case of antimony. *Physical Review Materials*, 2018, 2 (11), pp.114201. 10.1103/PhysRevMaterials.2.114201 . hal-01952951

HAL Id: hal-01952951

<https://hal.sorbonne-universite.fr/hal-01952951>

Submitted on 12 Jun 2019

HAL is a multi-disciplinary open access archive for the deposit and dissemination of scientific research documents, whether they are published or not. The documents may come from teaching and research institutions in France or abroad, or from public or private research centers.

L'archive ouverte pluridisciplinaire **HAL**, est destinée au dépôt et à la diffusion de documents scientifiques de niveau recherche, publiés ou non, émanant des établissements d'enseignement et de recherche français ou étrangers, des laboratoires publics ou privés.

Magnetoresistance of semi-metals: the case of antimony

Benoît Fauqué^{1,2,*}, Xiaojun Yang^{2,3}, Wojciech Tabis^{4,5}, Mingsong Shen⁶,
Zengwei Zhu⁶, Cyril Proust⁴, Yuki Fuseya^{2,7}, and Kamran Behnia^{2,†}

¹ JEIP, USR 3573 CNRS, Collège de France,
PSL Research University, 11, place Marcelin Berthelot,
75231 Paris Cedex 05, France.

² ESPCI ParisTech, PSL Research University CNRS,
Sorbonne Universités, UPMC Univ. Paris 6,
LPEM, 10 rue Vauquelin,
F-75231 Paris Cedex 5, France

³ School of Physics and Optoelectronics,
Xiangtan University, Xiangtan 411105, China.

⁴ Laboratoire National des Champs Magnétiques Intenses (LNCMI-EMFL),
CNRS, UGA, UPS, INSA, Grenoble/Toulouse, France

⁵ AGH University of Science and Technology,
Faculty of Physics and Applied Computer Science,
30-059 Krakow, Poland

⁶ Wuhan National High Magnetic Field Center and School of Physics,
Huazhong University of Science and Technology,
Wuhan 430074, China

⁷ Department of Engineering Science,
University of Electro-Communications,
Chofu, Tokyo 182-8585, Japan

(Dated: March 5, 2018)

Large unsaturated magnetoresistance has been recently reported in numerous semi-metals. Many of them have a topologically non-trivial band dispersion, such as Weyl nodes or lines. Here, we show that elemental antimony displays the largest high-field magnetoresistance among all known semi-metals. We present a detailed study of the angle-dependent magnetoresistance and use a semi-classical framework invoking an anisotropic mobility tensor to fit the data. A slight deviation from perfect compensation and a modest variation with magnetic field of the components of the mobility tensor are required to attain perfect fits at arbitrary strength and orientation of magnetic field in the entire temperature window of study. Our results demonstrate that large orbital magnetoresistance is an unavoidable consequence of low carrier concentration and the sub-quadratic magnetoresistance seen in many semi-metals can be attributed to field-dependent mobility, expected whenever the disorder length-scale exceeds the Fermi wavelength.

Detailed studies of magnetoresistance have been carried out in a large variety of systems ranging from ferromagnetic-metallic multilayer devices [1], manganite perovskites [2], and doped semi-conductors [3]. The large increase in the resistivity of semi-metals, which appears when the magnetic field is applied perpendicular to the orientation of the electric current has been known for a long time [4]. Recently, such a large orbital magnetoresistance has been observed in many dilute metals. The list includes three-dimensional Dirac systems (Cd₃As₂ [5]), Weyl semi-metals (WTe₂ [6], NbP [7] or WP₂ [8, 9], LaBi [10]), but also 'trivial' semi-metals (LaSb [11], gray arsenic [12]). Reporting on the large magnetoresistance in WTe₂, Ali *et al.* [6] contrasted its unsaturated B² behavior to the quasi-linear and eventually saturating high-field magnetoresistance of well-known semi-metals such as bismuth and graphite. Soon afterwards, WTe₂ was

identified as a type-II Weyl semimetal [13]. During the last three years, the link between amplitude and the field-dependence of magnetoresistance and its possible link to non-trivial electronic topology became a subject of debate and motivated numerous studies.

Here, we present the case of elemental antimony, another well-known semi-metal. Despite the remarkably high mobility of its bulk carriers [14] and its topologically non-trivial surface states [16], its large bulk magnetoresistance [15, 17] has never been studied in detail. Its carrier density of $n \simeq p \simeq 5.5 \times 10^{19} \text{ cm}^{-3}$ [18] is comparable to WTe₂ ($n \simeq p \simeq 6.6 \times 10^{19} \text{ cm}^{-3}$ [19]) and two orders of magnitude larger than bismuth ($n \simeq p \simeq 3 \times 10^{17} \text{ cm}^{-3}$ [24]). We show that in a reasonably clean Sb single crystal, a magnetic field of 56 T enhances resistivity by a factor of $\frac{\Delta\rho}{\rho_0} = 3 \times 10^6$. This is one order of magnitude higher than what was reported in WTe₂ [6], and comparable with what was observed in WP₂ [8]. The field dependence of magnetoresistance is close to (but slightly different from) quadratic. We present an angle-dependent study, with magnetic field kept perpendicular

*benoit.fauque@espci.fr
†kamran.behnia@espci.fr

to the applied current and rotating in three perpendicular crystalline planes (as in the case of bismuth [20]), and employ a semiclassical picture, based on distinct mobility tensors for electrons and holes, to explain the data. We show that by assuming slightly imperfect compensation, one can explain the finite Hall response. Taking into account a smooth field-induced reduction in mobility allows perfect fits to the non-quadratic magnetoresistance and the non-linear Hall resistivity at the same time. Thus, antimony becomes the first semi-metal whose extremely large magnetoresistance is totally explained by an extended semiclassical treatment for any arbitrary amplitude and orientation of magnetic field.

The two additional assumptions required to attain perfect fits bring new insight to the apparent diversity of semi-metallic magnetoresistance. Imperfect compensation caused by 1 part per million (ppm) of uncontrolled doping is barely noticeable when there is one hole and one electron per 10^4 atoms, that is when carrier density is in the range of 10^{19}cm^{-3} . But the same amount of uncontrolled doping has a much stronger signature when the carrier density is two orders of magnitude lower. This explains why the high-field magnetoresistance is close to quadratic in Sb and WTe_2 , but almost linear in Bi. The field-induced reduction in mobility can be caused by a disorder invisible to long-wavelength electrons at zero-field and becoming relevant in presence of magnetic field. Since the electron wave-function is smoothly squeezed by magnetic field, Raleigh scattering by extended defects becomes more efficient as the Landau levels are depopulated [21]. This provides a simple, but non-universal foundation for the field-induced decrease in mobility leading to the ubiquitous non-quadratic magnetoresistance.

Fig. 1a) presents the reported magnetoresistance of numerous semimetals at $B=9\text{T}$ and $T=2\text{K}$ (See [22] for details). The amplitude of field-induced enhancement in resistivity is plotted as a function of zero-field mobility, extracted from resistivity and carrier density: $\mu_0 = \frac{1}{\rho_0(n+p)e}$. Here, e is the charge of the electron, n and p are the electron and hole densities and ρ_0 the zero-field resistivity at $T=2\text{K}$. One can see that across more than three orders of magnitude, the MR of semi-metals (topological or not) roughly scales with their zero-field mobility. The higher the mobility, the larger the magnetoresistance. However, one can, also see that systematically $\frac{\Delta\rho}{\rho_0}$ is lower than $81 < \mu_0^2 >$, which is what is expected for 9T if the mobility was the same unique number relevant to the two (zero-field conductivity, $\sigma=e(n\mu_e + p\mu_h)$, and finite-field magnetoresistance).

Even the most ideally simple semimetal requires more complexity. Such a system would have a single electron-like and a single hole-like Fermi surface. The two pockets are isotropic with scalar mobilities of μ_e and μ_h . The semi-classic magnetoresistance of such a system would be $\frac{\Delta\rho}{\rho_0} = < \mu_m^2 > B^2$, where $\mu_m = \sqrt{\mu_e\mu_h}$. Note that the zero-field average mobility is $\mu_0 = \frac{n\mu_e + p\mu_h}{(n+p)}$. The two average mobilities are identical only when $n=p$ and

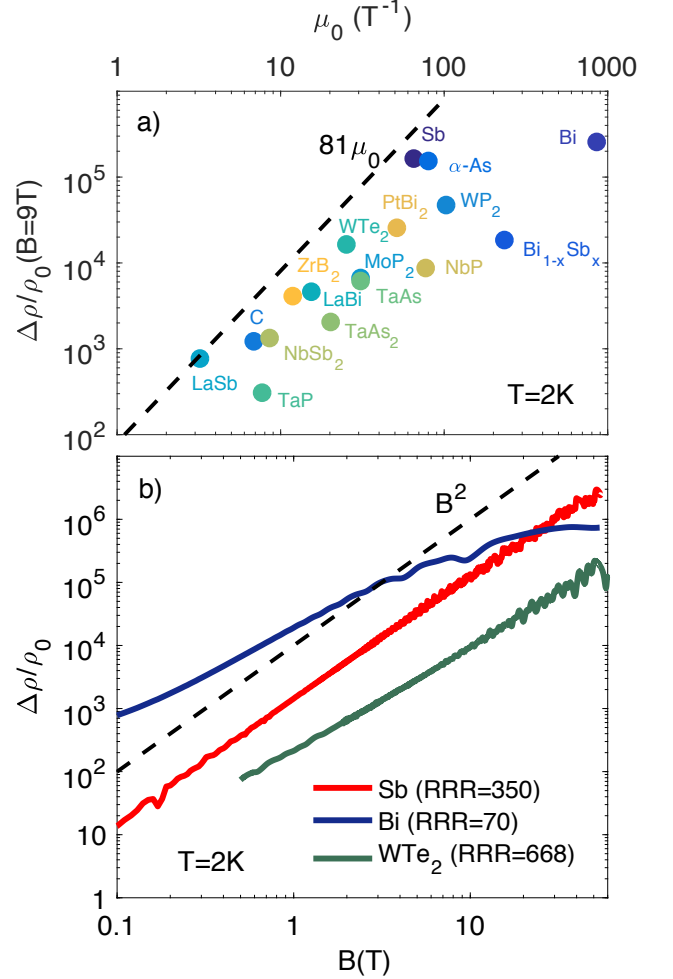


FIG. 1: a) Magnetoresistance of various semi-metals at $B=9\text{T}$ and $T=2\text{K}$ as a function of the mobility $\mu_0 = \frac{1}{\rho_0(n+p)e}$ where e is the charge of the electron, n and p are the electron and hole density and ρ_0 the zero field resistivity at 2K . μ_0 is expressed in $\text{Tesla}^{-1} = 10^4 \text{cm}^2 \cdot \text{V}^{-1} \cdot \text{s}^{-1}$ b) Magnetoresistance of elemental semi-metals antimony (j//trigonal and B//Bisectrix), bismuth (j//bisectrix and B//trigonal) and WTe_2 (j//a-axis and B//c-axis) at $T=2\text{K}$. RRR (Residual Resistivity Ratio) is equal to $\frac{\rho(T=300\text{K})}{\rho(2\text{K})}$.

$\mu_e = \mu_h$. However, μ_0 and μ_m remain of the same order of magnitude.

As seen in Fig. 1a, despite the discovery of numerous new compounds, the three elemental semimetals (Bi, Sb and As) are still those showing the largest magnetoresistance at 9T . Fig. 1b) compares the field dependence of magnetoresistance in bismuth, WTe_2 and antimony at $T=2\text{K}$ and $B \leq 56\text{T}$. One can see that it is close to B^2 in Sb and WTe_2 , but presents a lower exponent ($B^{1.5}$) and a tendency to saturation in bismuth. As a consequence, antimony surpasses bismuth above $\approx 25\text{T}$. Note that the amplitude of magnetoresistance in a given metal is not fixed and depends on the cleanness as we will discuss

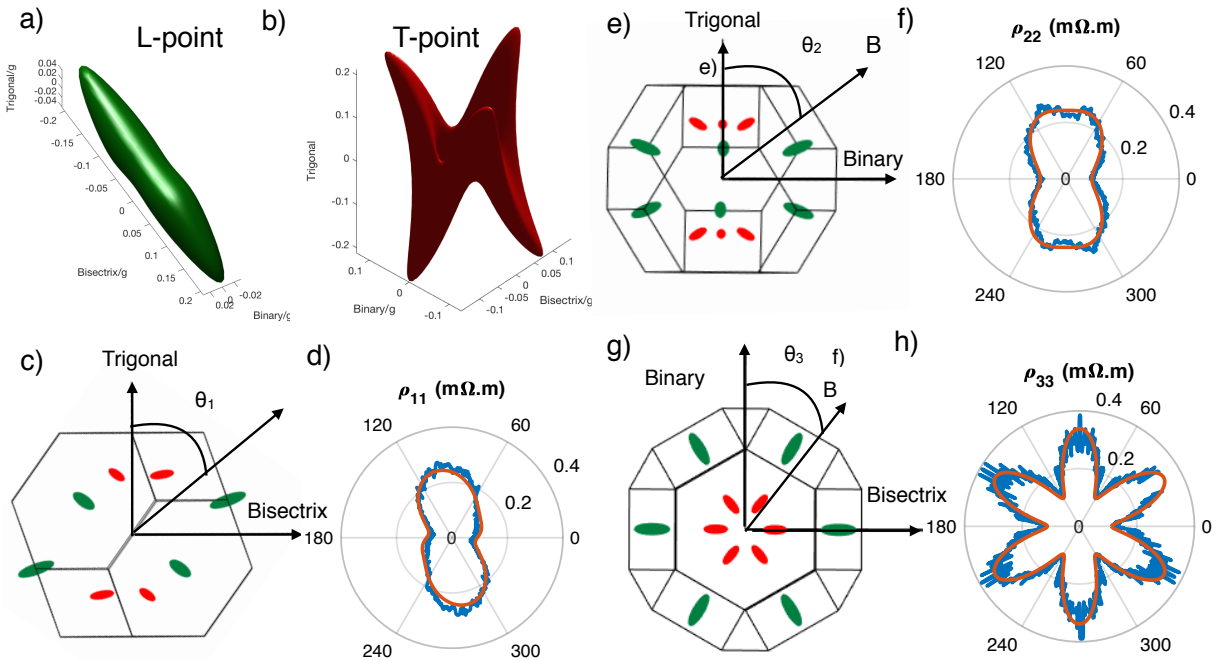


FIG. 2: Angular dependence of the magnetoresistance of antimony. a)-b) Electron and hole Fermi surface of antimony according to the Liu and Allen tight binding model. The unit of reciprocal length is $g = 1.461\text{\AA}^{-1}$. c) e) g) Sketch of the Brillouin zone and the Fermi surface of antimony projected in the three planes of rotation P_1 (Trigonal, Bisectrix), P_2 (Trigonal, Binary) and P_3 (Binary, Bisectrix). d) f) h) ρ_{ii} for $i=1,2$ and 3 in the three planes of rotation P_1 , P_2 and P_3 in blue at $T=2\text{K}$ and $B=12\text{T}$ (the electric current is applied along the crystal axis perpendicular to the rotating plane) measured on the same sample. The red line is a fit using a theoretical model described in the text.

below.

A more elaborate picture requires one to consider the tensorial nature of mobility. We attempted to achieve this by studying the angle dependence of ρ_{ii} in Sb when the magnetic field rotates in the plane perpendicular to the i -axis. Here, ($i=1,2,3$) refer to the binary, bisectrix and trigonal crystal axes. The three planes of rotations are P_1 =(trigonal, bisectrix), P_2 =(trigonal, binary) and P_3 =(binary, bisectrix), as in the case of bismuth [20].

The Fermi surface of Sb has been intensively studied by quantum oscillations [17, 18] and cyclotron resonance [23]. These studies have found that the density of electron and hole pockets is equal to $n=p=5.5 \times 10^{19} \text{cm}^{-3}$, within a precision of 1% [18]. In these studies, the Fermi surface was taken to be three equivalent electron pockets and six equivalent hole pockets. The electron pockets are quasi ellipsoids centered at the L-points of the Brillouin zone and reminiscent of the case of bismuth. The hole pockets consist of two groups of three pockets slightly off the T-points of the Brillouin zone and therefore non-isomorphic to the case of bismuth. According to the tight-binding model used by Liu and Allen [24], as discussed in the S. I. section C [22], the six hole pockets are interconnected around the T-point, as shown in Fig. 2b, a feature not explicitly mentioned previously [24].

The angle-dependence of the magnetoresistance at

$T=2\text{K}$ and $B=12\text{T}$ measured on the same sample for the three perpendicular planes of field rotation are presented in Fig.2d, f, h. In each case, the profile of $\rho_{ii}(\theta)$ reflects the symmetry of the projected profile of the Fermi surface components in that plane (Fig.2c, e, g). When the current is along the binary and the magnetic field rotates in the P_1 plane, there is only the inversion symmetry so that: $\rho_{11}(\theta)=\rho_{11}(\pi+\theta)$. When the current is along the bisectrix and a magnetic field rotates in P_2 plane, as a consequence of additional mirror symmetry, $\rho_{22}(\theta) = \rho_{22}(-\theta)$. Finally, when the current is along the trigonal and the field rotates in the P_3 plane, sixfold oscillations results as a consequence of the C_3 symmetry combined with the inversion symmetry. In contrast to bismuth [20, 25] we did not observe any field-induced loss of threefold symmetry (see section E of [22] for more details).

In order to extract the components of the mobility tensor for electrons and holes, we used the formalism developed first by the Mackey and Sybert [27] and then by Aubrey [28]. In this approach, the total conductivity is the sum of the contributions by each valley expressed as:

$$\hat{\sigma}_{e,h} = ne (\hat{\mu}_{e,h}^{-1} \mp \hat{B})^{-1} \quad (1)$$

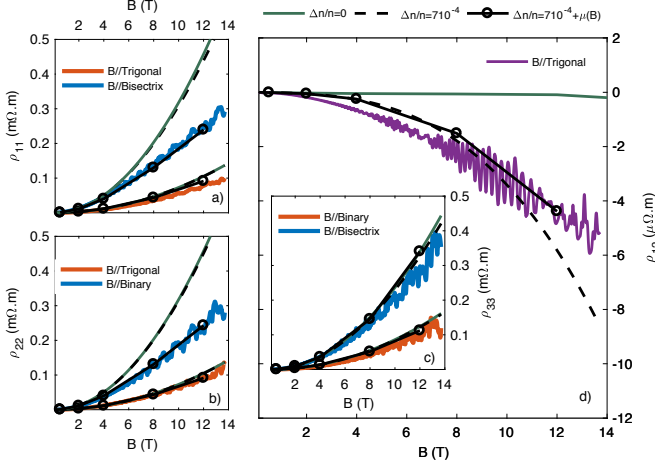


FIG. 3: Transverse magnetoresistance of Sb at $T=2\text{K}$ along the axes of high symmetry : a) $\rho_{11}(B)$ for B// trigonal (in blue) and B//bisectrix (in red), b) $\rho_{22}(B)$ for B// trigonal (in blue) and B//binary (in red) c) $\rho_{33}(B)$ for B//binary (in blue) and B//bisectrix (in red), d) ρ_{12} for B//trigonal (in purple). The green lines correspond to the Mackey and Sybert's model assuming no change in mobility tensors with the magnetic field and a perfect compensation ($\frac{\Delta n}{n}=0$). The dashed black lines correspond to the same model with a deviation from perfect compensation equal to $\frac{\Delta n}{n}=7\times 10^{-4}$ which allow to capture the Hall response. The black lines correspond to the same model with a field dependence mobility tensor (reported on Fig. 4b) and a deviation from perfect compensation $\frac{\Delta n}{n}=7\times 10^{-4}$.

where \hat{B} is defined as:

$$\hat{B} = \begin{pmatrix} 0 & -B_3 & B_2 \\ B_3 & 0 & -B_1 \\ -B_2 & B_1 & 0 \end{pmatrix} \quad (2)$$

Here, $\hat{\mu}_{e,h}$ is the mobility tensor of electrons and holes. B_1 , B_2 and B_3 are the projections of the magnetic field vector along the three principal axes. By employing this formalism, we could extract the components of the mobility tensor along the principal axes of the representative ellipsoids for electrons, μ_i , and holes, ν_i ($i=1, 2, 3$). Further details can be found in [22] section D.

We needed to add two ingredients to this formalism in order to substantially improve the fits. These were a slight departure from perfect compensation and taking into consideration the evolution of μ_i and ν_i with magnetic field. In this formalism, the Hall response is expected to be linear in the high-field regime ($\mu B \gg 1$) if the compensation is perfect. As illustrated in Fig.3 d), experimentally, this is not the case. The non-linear Hall resistivity can be captured by assuming a slight imbalance between hole and electron density, $\frac{\Delta n}{n} = \frac{p-n}{n}$. We find that the best agreement with data yields $\frac{\Delta n}{n} = 7 \times 10^{-4}$. This roughly corresponds to one defects per million unit cell, consistent with the 5N quality Sb powder used to grow the sample and with early galvanomet-

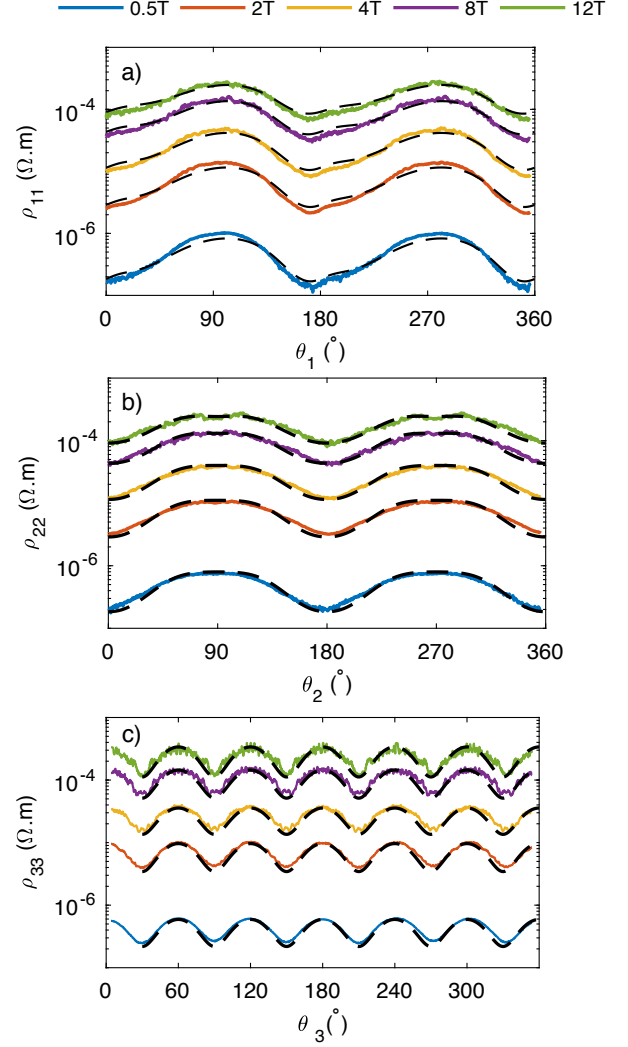


FIG. 4: Angular dependence of the magnetoresistance of Sb at $T=2\text{K}$ for $B=0.5\text{T}$ to 12T in the three plans of rotations a) P_1 , b) P_2 and c) P_3 . The dot lines are fits using the semi-classical model describes in the text.

ric measurements [15]. The consistency of our analysis is checked by comparing the field dependence of ρ_{11} , ρ_{22} and ρ_{33} (See Fig.3 a-d). One can see that imperfect compensation combined with a slight field-dependence of the components of the mobility tensor provides a satisfactory description of the overall field dependence of ρ_{11} , ρ_{22} , ρ_{33} and ρ_{12} .

Our best simultaneous fits of ρ_{11} , ρ_{22} and ρ_{33} at $T=2\text{K}$ and $B=12\text{T}$ are represented in red in Fig.2. We performed similar fits at different temperature and magnetic fields (see Fig.4) to obtain the magnitude of the components of the mobility tensors at any magnetic field and temperature in Fig.5. One can see that the temperature dependence closely tracks the temperature dependence of the zero-field mobility along the trigonal axis: $\mu_0[\rho_{33}] = \frac{1}{ne\rho_{33}(B=0)}$. At low temperature, the compo-

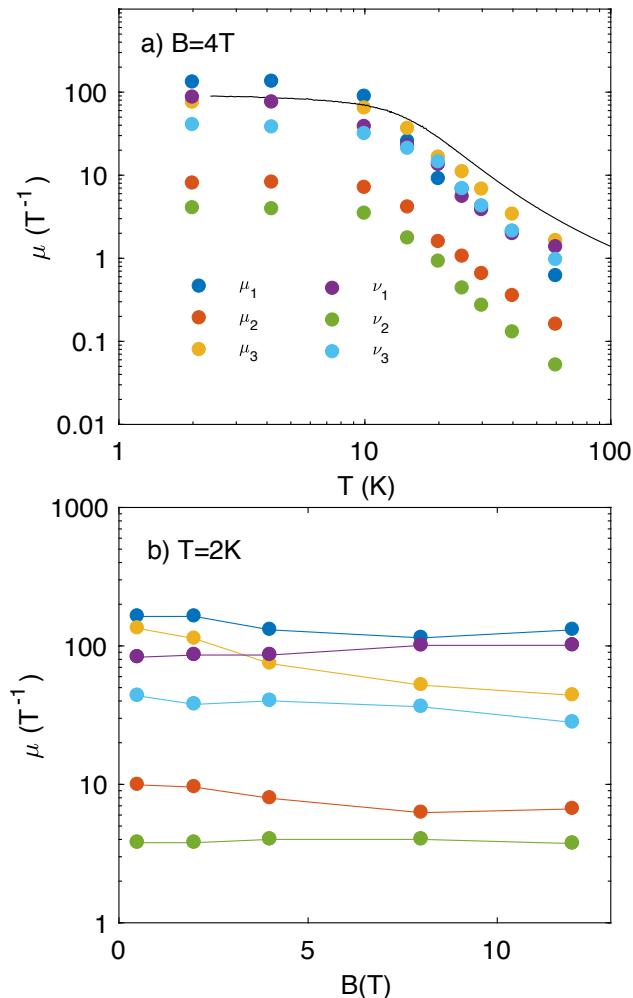


FIG. 5: Temperature and field dependence of mobility tensors of Sb : the hole and electron tensor component are respectively labelled (ν_1, ν_2, ν_3) , (μ_1, μ_2, μ_3) a) ν_i and μ_i for $i=1,2,3$ at $B=4\text{T}$ as function of temperature. The black line is the mobility deduced from the temperature dependence of ρ_{33} in the Drude picture b) Field dependence of μ_i and ν_i for $i=1,2,3$ at $T=2\text{K}$ deduced from the fit reported on Fig. 4

nents of the mobility tensor saturate. Above 10 K, they show a T^{-2} , like the one seen in bismuth[20] and attributed to inter-valley carrier-carrier scattering[26].

The mobility tensors and the mass tensors are linked by $\hat{\mu}_{e,h} = e\hat{\alpha}_{e,h} \cdot \hat{\tau}_{e,h}$. Here, $\hat{\alpha}$ and $\hat{\tau}$ share the same principal axes and $\hat{\alpha}$ is the inverse of the mass tensor. Its components are the cyclotron masses [23]. The anisotropy of the scattering rate is set by (and is attenuated compared to) the anisotropy of the effective mass(see section D of [22]).

The field dependence of the components of the mobil-

ity tensor is also instructive. When the field is swept from 0.5T to 12T, μ_1 , ν_1 , ν_2 are almost constant, but μ_2 and ν_3 decrease by a factor of 1.5 and μ_3 by a factor of 3. The fact that magnetic field does not affect in a similar manner among different components of the mobility tensor is a clue to the origin of the scattering process which becomes more effective in presence of magnetic field. The drastic decrease in μ_3 indicates that disorder in the orientation perpendicular to the cleaving planes becomes more significant with increasing field. Another piece of evidence is provided by contrasting samples with different levels of disorder. As presented in [22], the sub-quadratic aspect of magnetoresistance becomes more pronounced in dirtier samples where both the RRR (Residual Resistivity Ratio) and the Dingle mobility, μ_D are lower. A ratio of $\frac{\mu_0}{\mu_D}$ as large as 300 implies a significant role for small angle scattering. We thus identify long-range disorder as the ultimate source of sub-quadratic magnetoresistance.

In conclusion, we found a very large magnetoresistance in elemental antimony towering over most reported cases. We showed that the magnitude of the magnetoresistance at any temperature and magnitude or orientation of the magnetic field can be explained using a semi-classical framework with two additional ingredients, a weak deviation from perfect compensation and a field-dependent mobility tensor. The same framework can be used to address all other semi-metals. We conclude that because of slight imperfect compensation sub-quadratic magnetoresistance is unavoidable. In antimony or in WTe_2 , the carrier concentration is large enough to cover the role played by imperfect compensation, yet small enough to allow carriers to have a large mobility. This is the main reason behind its towering magnetoresistance. The phenomenological achievement reported here is only one step towards a microscopic theory. The challenge is to describe the anisotropic effect of magnetic field on carriers with a known dispersion in presence of a precise scattering potential. This would pin down the intrinsic limits of mobility in a given material.

Acknowledgments

This work is supported by the Agence Nationale de Recherche as a part of the QUANTUMLIMIT project, by the Fonds-ESPCI and by a grant attributed by the Ile de France regional council. We acknowledge support from the LNCMI, a member of the European Magnetic Field Laboratory(EMFL). BF acknowledges support from Jeunes Equipes de l'Institut de Physique du Collège de France (JEIP). YF is supported by JSPS KAKENHI grants 16K05437 and 15KK0155. We thank D. Carpentier for stimulating discussions.

[1] P. M. Levy, Giant magnetoresistance in magnetic layered and granular materials, *Solid State Phys.* **47**, 367 (1994).

[2] C. N. R. Rao and B. Raveau, Eds., *Colossal Magne-*

- toresistance, Charge Ordering and Related Properties of Manganese Oxides (World Scientific, Singapore,1998)
- [3] S. A. Solin, T. Thio, D. R. Hines, J. J. Heremans, Enhanced Room-Temperature Geometric Magnetoresistance in Inhomogeneous Narrow-Gap Semiconductors, *Science* **289**, 1530 (2000).
- [4] P. Kapitza, The study of the specific resistance of bismuth crystals and its change in strong magnetic fields and some allied problems, *Proc. R. Soc. A* **119**, 358 (1928).
- [5] Tian Liang, Quinn Gibson, Mazhar N. Ali, Minhao Liu, R. J. Cava and N. P. Ong, Ultrahigh mobility and giant magnetoresistance in the Dirac semimetal Cd_3As_2 , **14**,(280) *Nat. Mat.* (2015)
- [6] M. N. Ali and al., *Nature*, **514**, 205208 (2014)
- [7] C. Shekhar and al., Extremely large magnetoresistance and ultrahigh mobility in the topological Weyl semimetal candidate NbP, *Nat. Phys.*, **11**, 645649 (2015)
- [8] N. Kumar and al., Extremely high magnetoresistance and conductivity in the type-II Weyl semimetals WP_2 and MoP_2 , *Nat. Com.*, **8**, 1642 (2017)
- [9] R. Schonemann, N. Aryal, Q. Zhou, Y.-C. Chiu, K.-W. Chen, T. J. Martin, G. T. McCandless, J. Y. Chan, E. Manousakis, and L. Balicas, Fermi surface of the Weyl type-II metallic candidate WP_2 , *Phys. Rev. B* **96**, 121108 (2017)
- [10] S. Shanshan, W. Qi, G. Peng Jie, L. Kai, and L. Hechang, Large magnetoresistance in LaBi: origin of field-induced resistivity upturn and plateau in compensated semimetals, *New J. Phys.* **18**, 082002, (2016).
- [11] F. F. Tafti, Q. D. Gibson, S. K. Kushwaha, N. Haldolaarachchige, R. J. Cava, Consequences of breaking time reversal symmetry in LaSb: a resistivity plateau and extreme magnetoresistance, *Nat. Phys.* **12**, 272 (2016)
- [12] L. Zhao and al., Magnetotransport properties in a compensated semimetal gray arsenic, *Phys. Rev. B* **95**, 115119 (2017)
- [13] A. A. Soluyanov, D. Gresch, Z. Wang, Q. Wu, M. Troyer, X Dai and B. A. Bernevig, Type-II Weyl semimetals, *Nature* **527**, pages 495498 (2015)
- [14] B. N. Aleksandrov, V. V. Dukin, L.A. Maslova, and S. V. Tsvinsk, Effect of size and Temperature on the electric resistance of antimony single crystals, *Sov. Phys. JETP*, **34**, 125 (1972)
- [15] M. S. Bresler and N. A. Red'ko, Galvanomagnetic phenomena in antimony at low temperatures, *Soviet Physics JETP*, **34**, 149 (1972)
- [16] J. Seo, P. Roushan, H. Beidenkopf, Y. S. Hor, R. J. Cava and A. Yazdani, Transmission of topological surface states through surface barriers, *Nature* **466**, 343 (2010)
- [17] N. B. Brandt, E. A. Svistova and T. V. Gorskaya, Electrical resistance of antimony in a magnetic field up to 420kOe at liquid helium temperature, *Sov. Phys. JETP*, **26**, 745 (1968)
- [18] L. R. Windmiller, de Haasvan Alphen Effect and Fermi Surface in Antimony, *Phys. Rev.* **149**, 472 (1966)
- [19] Z. Zhu, X. Lin, J. Liu, B. Fauqué, Q. Tao, C. Yang, Y. Shi, and K. Behnia, Quantum Oscillations, Thermoelectric Coefficients, and the Fermi Surface of Semimetallic WTe_2 , *Phys. Rev. Lett.* **114**, 176601 (2015)
- [20] A. Collaudin, B. Fauqué, Y. Fuseya, W. Kang, and K. Behnia, Angle Dependence of the Orbital Magnetoresistance in Bismuth, *Phys. Rev. X* **5**, 021022 (2015)
- [21] J. C. W. Song, G. Refael, and P. A. Lee, Linear magnetoresistance in metals: guiding center diffusion in a smooth random potential, *Phys. Rev. B* **92**, 1-5 (2015)
- [22] The supplementary material can be found online.
- [23] W. R. Datars and J. Vanderkooy, Cyclotron resonance and the Fermi surface of antimony, *IBM J. Res. Dev.* **8**, **247** (1964).
- [24] Y. Liu and R. E. Allen, Electronic structure of the semimetals Bi and Sb, *Phys. Rev. B* **52**, 1566 (1995).
- [25] Z. Zhu, A. Collaudin, B. Fauqué, W. Kang and K. Behnia, Field-induced polarisation of Dirac valleys in bismuth, *Nat. Phys.* **8**, 89-94 (2012).
- [26] R. Hartman, Temperature dependence of the low-field galvanomagnetic coefficients of bismuth. *Phys. Rev.* **181**, 1070 (1969)
- [27] H. J. Mackey and J. R. Sybert, Magnetoconductivity of a Fermi Ellipsoid with Anisotropic Relaxation Time, *Phys. Rev.*, **180**, 679 (1969)
- [28] J. E. Aubrey, Magnetoconductivity tensor for semimetals, *J. Phys. F* **1**, 493 (1971)